International Journal of Minerals, Metallurgy and Materials
Volume 21, Number 2, February 2014, Page 131
DOI: 10.1007/s12613-014-0875-z

Isothermal reduction of titanomagnetite concentrates containing coal

Tu Hu[1,2], *Xue-wei Lü*[1], *Chen-guang Bai*[1], *and Gui-bao Qiu*[1]

1) College of Materials Science and Engineering, Chongqing University, Chongqing 400044, China
2) Faculty of Metallurgical and Energy Engineering, Kunming University of Science and Technology, Kunming 650093, China

(Received: 9 September 2013; revised: 29 October 2013; accepted: 3 November 2013)

Abstract: The isothermal reduction of the Panzhihua titanomagnetite concentrates (PTC) briquette containing coal under argon atmosphere was investigated by thermogravimetry in an electric resistance furnace within the temperature range of 1250-1350°C. The samples reduced in argon at 1350°C for different time were examined by X-ray diffraction (XRD) analysis. Model-fitting and model-free methods were used to evaluate the apparent activation energy of the reduction reaction. It is found that the reduction rate is very fast at the early stage, and then, at a later stage, the reduction rate becomes slow and decreases gradually to the end of the reduction. It is also observed that the reduction of PTC by coal depends greatly on the temperature. At high temperatures, the reduction degree reaches high values faster and the final value achieved is higher than at low temperatures. The final phase composition of the reduced PTC-coal briquette consists in iron and ferrous-pseudobrookite ($FeTi_2O_5$), while $Fe_{2.75}Ti_{0.25}O_4$, $Fe_{2.5}Ti_{0.5}O_4$, $Fe_{2.25}Ti_{0.75}O_4$, ilmenite ($FeTiO_3$) and wustite (FeO) are intermediate products. The reaction rate is controlled by the phase boundary reaction for reduction degree less than 0.2 with an apparent activation energy of about 68 $kJ\cdot mol^{-1}$ and by three-dimensional diffusion for reduction degree greater than 0.75 with an apparent activation energy of about 134 $kJ\cdot mol^{-1}$. For the reduction degree in the range of 0.2-0.75, the reaction rate is under mixed control, and the activation energy increases with the increase of the reduction degree.

Keywords: titanomagnetite; carbothermal reduction; thermogravimetric analysis; kinetics

1. Introduction

Vanadium-titanium-bearing magnetite of Panzhihua, China, is a complex iron ore composed by the coexistence of vanadium and titanium that accounts for more than 90% of the titanium reserves in China. Most of the titanomagnetite concentrates are now used as the main materials for the blast furnace process in Panzhihua area. Most of the iron and, partly, vanadium can be reduced into the hot metal; however, almost all of the titanium remains in the slag, forming a high-titanium slag with contents of TiO_2 varying from 22wt% to 25wt%. There is no an appropriate and economic method to deal with such slag [1] so far. Recently, most of the studies focused on developing an alternative route to use the titanomagnetite concentrates, highlighting the rotary hearth furnace (RHF) process, which involves the reduction of composite briquette of titanomagnetite concentrates with coal, and the smelting of the reduced sample in an electric arc furnace.

The direct reduction of Panzhihua titanomagnetite concentrates (PTC) by solid reductants has been widely studied for many decades [1-6]. It was found that the reduction of titanomagnetite was slower than that of magnetite due to the different crystal structures and the presence of titanium, resulting in a higher thermodynamic stability of titanomagnetite [7-13]. Here, the kinetics of the carbothermal reduction of PTC was studied by using thermogravimetry. During the heating process of the composite briquette of PTC and coal, the mass loss is caused by the release of volatiles from coal, carbon loss, and removal of oxygen by reduction. A pseudo-kinetic parameter, fraction of reaction (f), has been used to measure the reaction rate. It has been observed that the estimation of the pseudo-kinetic parameter (f) is not identical to that of the degree of reduction and can only provide a rough estimate of the extent and characteristics of the reduction [14].

In the present work, the isothermal reduction of PTC by coal was investigated by thermogravimetry, and the reduction degree was used to analyze the kinetic data.

Corresponding author: Tu Hu E-mail: hutu1219@126.com

2. Experimental

2.1. Specimen preparation and experimental procedures

The chemical compositions and size distributions of the raw materials were examined and are presented in Tables 1-3. Fig. 1 shows the X-ray diffraction (XRD) pattern of PTC. The mineral compositions were mostly titanomagnetite, magnetite, and ilmenite. Two types of specimens were prepared. One type contained PTC and coal, and the other contained alumina particles and coal. For the former type, the PTC was mixed homogenously with the coal with a molar ratio ($C_{\text{fixed}}/O_{(\text{bonded with Fe})}$) of 1.2. The mixture was made into spheroid briquettes at 15 MPa with a briquette maker. The diameter of the briquette was about 30 mm, and the total mass of the sample was about 25 g. The other type of briquette made of coal and alumina particles, which has the same amount of coal and the same geometries as the briquette made of PTC and coal, was made under the same conditions. All the briquettes were dried at 120°C for 6 h before the reduction experiments.

Table 1. Chemical composition of Panzhihua titanomagnetite concentrates (PTC) and coal wt%

PTC								Coal			
TFe	FeO	TiO_2	V_2O_5	SiO_2	CaO	MgO	Al_2O_3	C	Volatile	Ash	S
52.62	32.00	12.00	0.60	4.20	1.30	2.60	3.90	81.95	6.95	10.41	0.69

Table 2. Size distribution of Panzhihua titanomagnetite concentrates (PTC)

Diameter / μm	< 74	74-80	80-96	96-109	109-120	120-150	> 150	Total
Content / wt%	88.40	3.26	4.20	1.86	1.81	0.32	0.15	100

Table 3. Size distribution of coal

Diameter / μm	< 100	150-180	180-250	250-550	550-1700	> 1700	Total
Content / wt%	20.80	51.34	14.81	9.87	2.00	1.18	100

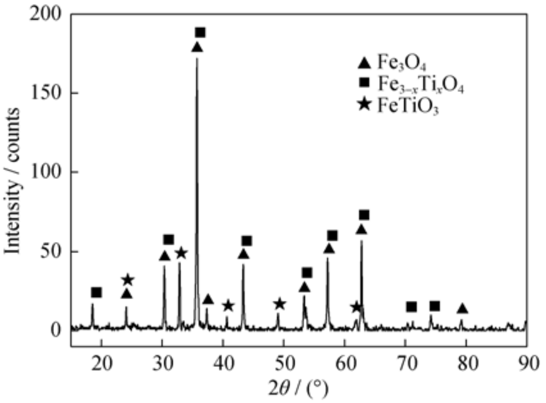

Fig. 1. X-ray diffraction pattern of Panzhihua titanomagnetite concentrates (PTC).

The isothermal reductions of the PTC with coal were carried out in a vertical electric resistance furnace, whose schematic is shown in Fig. 2. A briquette was loaded in a basket made of nichrome wire and hanged up to the furnace. The furnace was purified by blowing argon at a high rate before each experiment and, then, the flow rate of argon was kept at 1 L·min^{-1}. The basket with the briquette was loaded down quickly into the hot zone of the furnace when the furnace temperature reached the desired value. The mass of the briquette was measured and recorded continuously until the mass became constant. The reduced briquette was cooled in argon quickly after the sample was taken out from the furnace. Two types of briquettes were heated under the same experimental conditions at each temperature. Three identical experiments were performed for each time-temperature pair, and the averaged mass loss was used.

The phase transformations of PTC during the reduction at 1350°C by coal were investigated by XRD, which was conducted using a Cu K_α source.

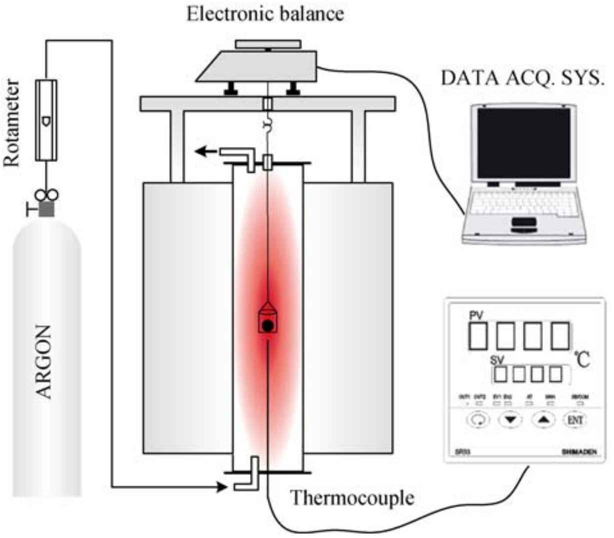

Fig. 2. Schematic of the experimental system.

2.2. Determination of the degree of reduction

The degree of reduction (R) is usually defined as the ratio of the accumulated mass of oxygen removed at time t to the total mass of removable oxygen bonded with iron, which is given by

$$R = \frac{\Delta M_{\mathrm{O}}^{t}}{\Delta M_{\mathrm{O}}} \tag{1}$$

where $\Delta M_{\mathrm{O}}^{t}$ (g) is the mass of oxygen removed at time t during the isothermal heating process of the briquette, and ΔM_{O} (g) is the total mass of removable oxygen bonded with iron in the briquette. The mass loss of the PTC-coal briquette during heating consists of the volatile emission, carbon, and oxygen loss upon reduction. Therefore, Eq. (1) can be re-written as

$$R = \frac{\Delta M_{\Sigma}^{t} - \Delta M_{\mathrm{C}}^{t} - \Delta M_{\mathrm{V}}^{t}}{\Delta M_{\mathrm{O}}} \tag{2}$$

where ΔM_{Σ}^{t} (g) is the mass loss of the PTC-coal briquette at time t, $\Delta M_{\mathrm{C}}^{t}$ (g) is the mass loss of carbon at time t, and $\Delta M_{\mathrm{V}}^{t}$ (g) is the mass loss of the volatile emission at time t. The value of $\Delta M_{\mathrm{V}}^{t}$ can be measured according to the mass loss of the Al_2O_3-coal briquette in argon at time t, and here, it is represented by $\Delta M_{\mathrm{AC}}^{t}$ (g).

It has been established that there is little CO_2 during the reduction of the PTC-coal briquette at temperature higher than 1000°C, due to the drastic carbon gasification reaction by CO_2 [9]. Therefore, in present study, the reduction of iron oxides by carbon at high temperature can be generally represented by

$$\mathrm{Fe}_x\mathrm{O}_y + \mathrm{C} = \mathrm{Fe}_x\mathrm{O}_{y-1} + \mathrm{CO} \tag{3}$$

Therefore,

$$\Delta M_{\mathrm{C}}^{t} = \frac{12}{16}\Delta M_{\mathrm{O}}^{t} \tag{4}$$

Replacing $\Delta M_{\mathrm{C}}^{t}$ and $\Delta M_{\mathrm{V}}^{t}$ with $\frac{12}{16}\Delta M_{\mathrm{O}}^{t}$ and $\Delta M_{\mathrm{AC}}^{t}$ in Eq. (2), respectively, and combining Eq. (2) with Eq. (1), the degree of reduction can be expressed as

$$R = \frac{4}{7} \times \frac{\Delta M_{\Sigma}^{t} - \Delta M_{\mathrm{AC}}^{t}}{\Delta M_{\mathrm{O}}} \tag{5}$$

2.3. Methods for the evaluation of the activation energy

The reaction rate can be generally expressed by Eq. (6) [15]:

$$\frac{\mathrm{d}\alpha}{\mathrm{d}t} = k(T) f(\alpha) \tag{6}$$

where α is the degree of conversion, t the time, T the temperature, $k(T)$ the rate constant, and $f(\alpha)$ the pattern function determined by the kinetic model. The kinetic model may take various forms, some of which are shown in Table 4. The integral form of Eq. (6) is generally used for evaluating the activity energy under isothermal conditions, which is given by

$$g_i(\alpha) = k_j(T_i)t \tag{7}$$

where $g_i(\alpha) = \int_0^{\alpha} [f_j(\alpha)]^{-1} \mathrm{d}\alpha$ is the integral form of the kinetic model j (Table 4). The rate constant can be determined from the slope of the plot of $g_i(\alpha)$ versus t. For an appropriate kinetic model, the rate constants are evaluated at several temperatures $T_i T_i$, and the activation energy is determined using the Arrhenius equation in its logarithmic form, which is given as follows:

$$\ln k_j(T_i) = \ln A_j - \frac{E_j}{RT_i} \tag{8}$$

Table 4. Set of kinetic models commonly applied to describe solid state reactions

No.	Model	$f(\alpha)$	$g(\alpha)$
1	$D_1(\alpha)$	$\frac{1}{2}\alpha^{-1}$	α^2
2	$D_2(\alpha)$	$[-\ln(1-\alpha)]^{-1}$	$(1-\alpha)\ln(1-\alpha)+\alpha$
3	$D_3(\alpha)$	$\frac{3}{2}\left[1-(1-\alpha)^{1/3}\right]^{-1}(1-\alpha)^{2/3}$	$\left[1-(1-\alpha)^{1/3}\right]^2$
4	$D_4(\alpha)$	$\frac{3}{2}\left[(1-\alpha)^{1/3}-1\right]^{-1}$	$\left(1-\frac{2}{3}\alpha\right)-(1-\alpha)^{2/3}$
5	$F_1(\alpha)$	$1-\alpha$	$-\ln(1-\alpha)$
6	$R_2(\alpha)$	$2(1-\alpha)^{1/2}$	$1-(1-\alpha)^{1/2}$
7	$R_3(\alpha)$	$3(1-\alpha)^{2/3}$	$1-(1-\alpha)^{1/3}$
8	$A_2(\alpha)$	$2\left[-\ln(1-\alpha)^{1/2}\right](1-\alpha)$	$[-\ln(1-\alpha)]^{1/2}$
9	$A_3(\alpha)$	$3\left[-\ln(1-\alpha)^{2/3}\right](1-\alpha)$	$[-\ln(1-\alpha)]^{1/3}$

To obtain the most appropriate kinetic model, α can be plotted as a function of the dimensionless reduction time term t/t_{α} for each model and the experimental data, where t_{α} is the time required to reach a specified degree of conversion (e.g., $\alpha = 0.8$). The kinetic model by which the experimental data is well fitted is regarded as the most appropriate one. This method, the so-called model-fitting method, is widely applied in solid-state kinetics [16-17].

Only a single average value of the activation energy for an overall process can be obtained by the model-fitting method. It is difficult to obtain the activation energy if the experimental data cannot be fitted well by any of the reaction models, which reveals the complexity of the reaction mechanism. This can be avoided by using the model-free isoconversional method, which allows the activation energy to be determined as a function of the degree of conversion and without any kinetic model assumption [15].

For the model-free isoconversional method, Eqs. (7) and (8) can be combined to eliminate $k_j(T_i)$ to obtain the following equation:

$$\ln t_{\alpha,i} = \ln\left[\frac{A_\alpha}{g(\alpha)}\right] + \frac{E_\alpha}{R'T_i} \tag{9}$$

where R' is the gas constant, A_α is the pre-exponential factor, and $t_{\alpha,i}$ is the time required to reach a specified extent of conversion at temperature T_i. E_α represents the activation energy at a specified α and is evaluated from the slope of the plot of $\ln t_{\alpha,i}$ against T_i.

In this study, both the model-fitting and model-free methods were used to evaluate the apparent activation energy of the isothermal reduction of PTC by coal, and the degree of conversion (α) was substituted for the degree of reduction (R).

3. Results and discussion

3.1. Effect of the temperature on the carbothermal reduction of PTC

The mass loss of the PTC-coal briquette and Al_2O_3-coal briquette during reduction at different temperatures are shown in Fig. 3. There is little difference in the mass loss of Al_2O_3-coal briquettes heated at different temperatures because the volatilization rate of the volatiles in coal is very fast at the involved temperatures. According to the mass loss of briquettes, the degree of reduction of the PTC-coal briquette was calculated. The curves of reduction degree as a function of time for the PTC-coal briquettes at different temperatures are shown in Fig. 4. The reduction rate was very fast at the early stage and, then, it became slow and decreased gradually to the end of the reduction process. At the early stage, the reduction of magnetite to iron mainly occurred, and the carbon gasification by CO_2 was very fast, resulting in a high reaction rate at this stage. While the reduction proceeded, the reduction of titanium bearing iron oxides, whose reaction rate is slower than that of iron oxides, became the main reduction reaction, in which the carbon content was decreased due to the high consumption at the early stage. Therefore, the reduction rate decreased at the later stage.

It is also observed that the reduction of PTC by coal greatly depends on the temperature. For higher temperatures, the reduction degree reaches high values faster and the final value achieved is higher. This can be attributed to the higher heat transfer rate at higher temperatures. It is widely accepted that the mechanism of carbothermic reduction of iron oxides is a two-stage mechanism involving the participation of gaseous intermediates (e.g., CO and CO_2) according to the following equations:

$$Fe_xO_y + CO = Fe_xO_{y-1} + CO_2 \tag{10}$$

$$CO_2 + C = 2CO \tag{11}$$

The endothermic carbon gasification reaction plays an important role in the carbothermal reduction of iron oxides. During reduction, the high heat transfer rate induces the increase of the rate of gasification reaction and, thus, of the reduction rate. A high sintering rate of the oxides at high temperatures, enhancing the heat transfer inside the briquette, could also be responsible.

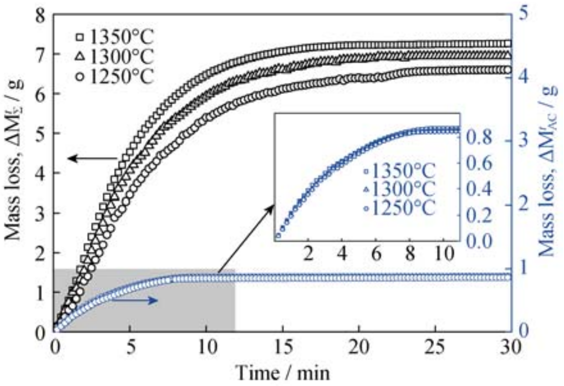

Fig. 3. Mass losses of Panzhihua titanomagnetite concentrates (PTC)-coal briquette and Al_2O_3-coal briquette during reduction at different temperatures.

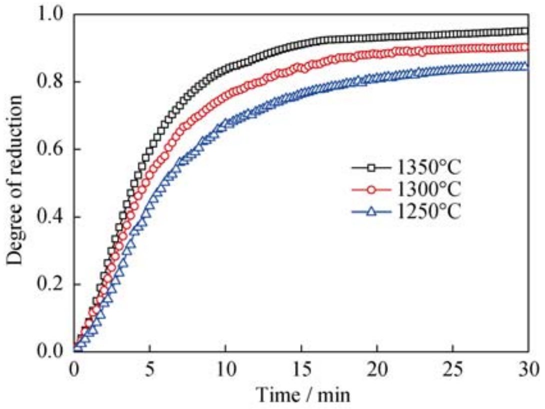

Fig. 4. Degree of reduction *vs.* reduction time for Panzhihua titanomagnetite concentrates (PTC)-coal briquettes reduced at different temperatures.

3.2. Phase transitions of the isothermal reduction of PTC by coal

The briquettes were heated at 1350°C for different time periods, and the reduced samples were examined by XRD, the patterns of which are shown in Fig. 5. The main phases of the sample reduced for 3 min are magnetite (Fe_3O_4), wustite (FeO), metallic iron, ilmenite ($FeTiO_3$), and titanomagnetite ($Fe_{2.75}Ti_{0.25}O_4$). Traces of $Fe_{2.5}Ti_{0.5}O_4$ were observed after 7 min. $Fe_{2.25}Ti_{0.75}O_4$ appeared in the sample reduced for 10 min. Wustite (FeO) and ilmenite ($FeTiO_3$) disappeared in the samples heated for 13 and 19 min, respectively. Traces of ferrous-pseudobrookite ($FeTi_2O_5$) were detected in the XRD pattern of the sample heated for 19 min. It is noticed that ulvospinel (Fe_2TiO_4) was not detected in the reduced samples because the ulvospinel formed during the heating process is quickly further reduced to metallic iron and ilmenite.

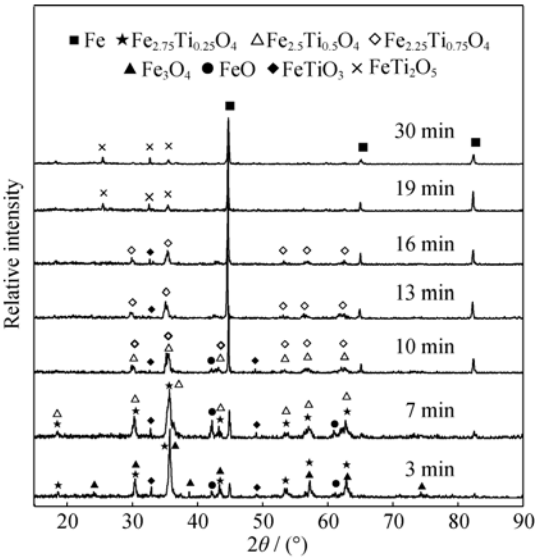

Fig. 5. X-ray diffraction patterns of Panzhihua titanomagnetite concentrates (PTC)-coal briquettes reduced at 1350°C for different time periods.

$Fe_{2.75}Ti_{0.25}O_4$, $Fe_{2.5}Ti_{0.5}O_4$, and $Fe_{2.25}Ti_{0.75}O_4$ are three different forms of titanomagnetite ($Fe_{3-x}Ti_xO_4$), which can be written as $3Fe_3O_4{\cdot}Fe_2TiO_4$, $Fe_3O_4{\cdot}Fe_2TiO_4$, and $Fe_3O_4{\cdot}3Fe_2TiO_4$, respectively. The phase transformation from $3Fe_3O_4{\cdot}Fe_2TiO_4$ to $Fe_3O_4{\cdot}3Fe_2TiO_4$ indicates that the proportion of magnetite (Fe_3O_4) in the solid solution $Fe_{3-x}Ti_xO_4$ of magnetite (Fe_3O_4) and ulvospinel (Fe_2TiO_4) decreases during the heating process, according to the following reactions:

$$3Fe_3O_4 \cdot Fe_2TiO_4 + 2CO(C) = Fe_3O_4 \cdot Fe_2TiO_4 + 6FeO + 2CO_2(CO) \quad (12)$$

$$3(Fe_3O_4 \cdot Fe_2TiO_4) + 2CO(C) = Fe_3O_4 \cdot 3Fe_2TiO_4 + 6FeO + 2CO_2(CO) \quad (13)$$

$$Fe_3O_4 \cdot 3Fe_2TiO_4 + CO(C) = 3Fe_2TiO_4 + 3FeO + CO_2(CO) \quad (14)$$

Based on the XRD analysis, as shown in Fig. 6, the phase transitions of PTC during the isothermal carbothermal reduction under the present conditions can be suggested.

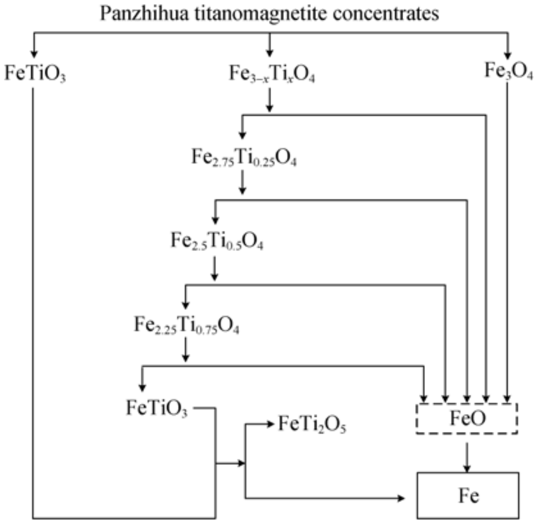

Fig. 6. Phase transitions of Panzhihua titanomagnetite concentrates (PTC) during carbothermal reduction at 1350°C.

3.3. Evaluation of the activation energy

To ascertain the most appropriate reaction model for using the model-fitting method, the experimental results were evaluated against the standard reduced time plots of the reaction models listed in Table 4. The results are shown in Fig. 7, in which the dashed curve corresponds to the data resulting from the average of three isothermal experiments performed at 1250, 1300, and 1350°C. It is found that the data cannot be entirely fitted by any of the reaction models, which reveals the complexity of the carbothermal reduction of PTC and indicates that the traditional model-fitting method for the activation energy evaluation is not feasible in this case. However, R values less than 0.2 fit well into the three-dimensional phase boundary reaction model (R_3) and R values greater than 0.75 fit well into the three-dimensional diffusion model (D_3). This indicates a change in the mechanism during the reduction of the PTC-coal briquette. It is suggested that the reaction rate is controlled by the phase boundary reaction at the first stage and by the three-dimensional diffusion at the final stage. At the second stage, the reaction rate is under the mixed control of phase boundary reaction and three-dimensional diffusion.

The apparent activation energy of the carbothermal reduction of iron oxides is generally a composite value determined by the activation energies of various reactions and by their influence on the overall reaction rate. Even if the temperature is kept constant, the relative contributions of the elementary steps into the overall reaction rate vary with the reduction degree, ultimately resulting in a dependence of the effective activation energy on the degree of reduction.

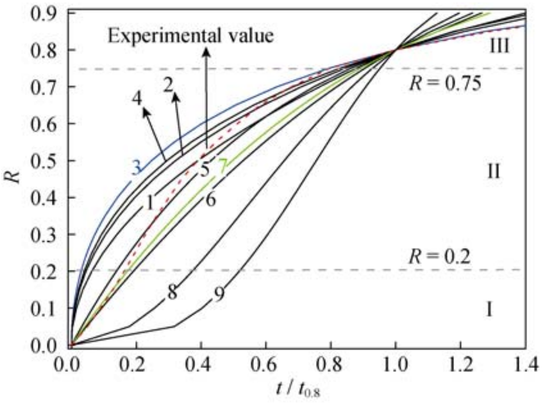

Fig. 7. Reduced time plots for the reaction models (solid curves 1-9 are obtained using kinetic models as enumerated in Table 4) and isothermal experimental data for PTC carbothermal reduction. The dashed curve corresponds to the data averaged from three isothermal experiments performed at 1250, 1300, and 1350°C.

Fig. 8 shows the dependency of E_R on R obtained using the model-free isoconversional method. For R less than 0.2, the activation energy is almost constant (~68 kJ·mol^{-1}). With the progress of the reduction, for R greater than 0.2, the activation energy increases gradually because the reduction of titanium bearing oxides, which are more difficult to reduce than magnetite and wustite, becomes dominant at increasing R. Moreover, the reactants are covered by the reduced product, resulting in the reduction occurring through the diffusion of gaseous species. When the degree of reduction is up to 0.75, the activation energy is constant (134 kJ·mol^{-1}), indicating that diffusion becomes the rate-controlling step. This is consistent with the observation in Fig. 7.

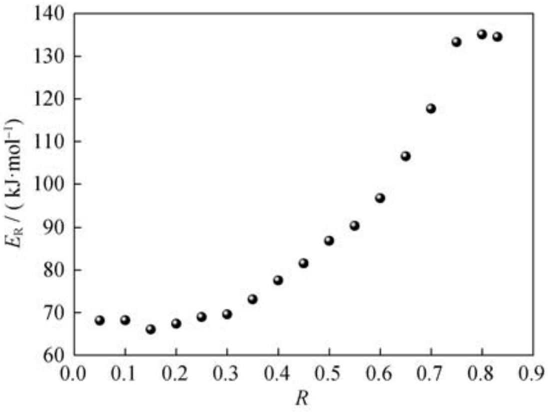

Fig. 8. Dependency of the activation energy on the degree of reduction determined using the model-free isoconversional method.

4. Conclusions

The isothermal reductions of Panzhihua titanomagnetite concentrates with coal were investigated by thermogravimetry in argon atmosphere at 1250, 1300, and 1350°C. The following conclusions are obtained.

(1) The reduction rate is very fast at the early stage. Then, at the later stage, the reduction rate becomes slow and decreases gradually to the end of the reduction. The reduction of PTC by coal depends greatly on the temperature. For higher temperatures, the reduction degree reaches high values faster, and the final value achieved is high.

(2) The PTC is reduced to iron at 1350°C in argon atmosphere along a stepwise sequence with $Fe_{2.75}Ti_{0.25}O_4$, $Fe_{2.5}Ti_{0.5}O_4$, $Fe_{2.25}Ti_{0.75}O_4$, ilmenite ($FeTiO_3$), wustite (FeO), and ferrous-pseudobrookite ($FeTi_2O_5$).

(3) The reduction rate is controlled by a phase boundary reaction for R less than 0.2 with an apparent activation energy of about 68 kJ·mol^{-1} and by three-dimensional diffusion for R greater than 0.75 with an apparent activation energy of about 134 kJ·mol^{-1}. For R in the range from 0.2 to 0.75, the reaction rate is under a mixed control and the apparent activation energy increases with increasing reduction degree.

Acknowledgements

This work was financially supported by the Major Program of National Natural Science Foundation of China (Nos. 51090383 and 51090382) and the Scholarship Award for Excellent Doctoral Student granted by the Ministry of Education of China (No. 0903005109081-8).

References

[1] D.S. Chen, L.N. Wang, T. Qi, and B. Song, Study on preoxidation of vanadium-bearing titanomagnetite concentrates, *J. Hunan Univ. Sci. Technol. Nat. Sci.*, 26(2011), No. 3, p. 95.

[2] Z.J. Liu, G.Q. Yang, Q.G. Xue, J.L. Zhang, and T.J. Yang, Research on direct reduction of coal-containing pellets of vanadic-titanomagnetite by rotary hearth furnace, *Chin. J. Process Eng.*, 9(2009), No. 1, p. 51.

[3] L.H. Zhou, D.P. Tao, M.X. Fang, F.H. Zeng, and X. Pu, Carbothermic reduction of V-Ti magnetite ore, *Chin. J. Rare Met.*, 33(2009), No. 3, p. 406.

[4] G.H. Zhang, Z. Yan, Y.J. Feng, M. Guo, X.D. Wang, L.F. Li, and G.Z. Zhou, Reduction kinetics of vanadic titanomagnetite in Panzhihua, *J. Chin. Rare Earth Soc.*, 26(2008), p. 210.

[5] X. Xue, Research on direct reduction of vanadic titanomagnetite, *Iron Steel Vanadium Titanium*, 28(2007), No. 3, p. 37.

[6] Y.Z. Lan and C.P. Liu, Kinetics of carbon catalytic reduction of titanomagnetite concentrate, *Acta Metall. Sin.*, 32(1996), No. 5, p. 502.

[7] E. Park and O. Ostrovski, Reduction of titania-ferrous ore by

hydrogen, *ISIJ Int.*, 44(2004), No. 6, p. 999.

[8] E. Park and O. Ostrovski, Reduction of titania-ferrous ore by carbon monoxide, *ISIJ Int.*, 43(2003), No. 9, p. 1316.

[9] T. Hu, X.W. Lv, C.G. Bai, Z.G. Lun, and G.B. Qiu, Reduction behavior of Panzhihua titanomagnetite concentrates with coal, *Metall. Mater. Trans. B*, 44(2013), No. 2, p. 252.

[10] X.W. Lv, Z.G. Lun, J.Q. Yin, and C.G. Bai, Carbothermic reduction of vanadium titanomagnetite by microwave irradiation and smelting behavior, *ISIJ Int.*, 53(2013), No. 7, p. 1115.

[11] H.Y. Sun, X.J. Dong, X.F. She, Q.G. Xue, and J.S. Wang, Solid state reduction of titanomagnetite concentrate by graphite, *ISIJ Int.*, 53(2013), No. 4, p. 564.

[12] H.Y. Sun, J.S. Wang, Y.H. Han, X.F. She, and Q.G. Xue, Reduction mechanism of titanomagnetite concentrate by hydrogen, *Int. J. Miner. Process.*, 125(2013), No. 12, p. 122.

[13] J.L. Zhang, X.D. Xing, M.M. Cao, K.X. Jiao, C.L. Wang, and S. Ren, Reduction kinetics of vanadium titano-magnetite carbon composite pellets adding catalysts under high temperature, *J. Iron Steel Res. Int.*, 20(2013), No. 2, p. 1.

[14] S.K. Dey, B. Jana, and A. Basumallick, Kinetics and reduction characteristics of hematite-noncoking coal mixed pellets under nitrogen gas atmosphere, *ISIJ Int.*, 33(1993), No. 7, p. 735.

[15] S. Vyazovkin and C.A. Wight, Model-free and model-fitting approaches to kinetic analysis of isothermal and nonisothermal data, *Thermochim. Acta*, 340-341(1999), p. 53.

[16] M.E. Brown, D. Dollimore, and A.K. Galwey, Reactions in the solid state, [in] *Comprehensive Chemical Kinetics*, Elsevier, 22(1980), p. 347.

[17] J.H. Sharp, G.W. Brindley, and B.N. Narahari, Numerical data for some commonly used solid state reaction equations, *J. Am. Ceram. Soc.*, 49(1966), No. 7, p. 379.